RSC Advances

ROYAL SOCIETY OF CHEMISTRY

www.rsc.org/advances

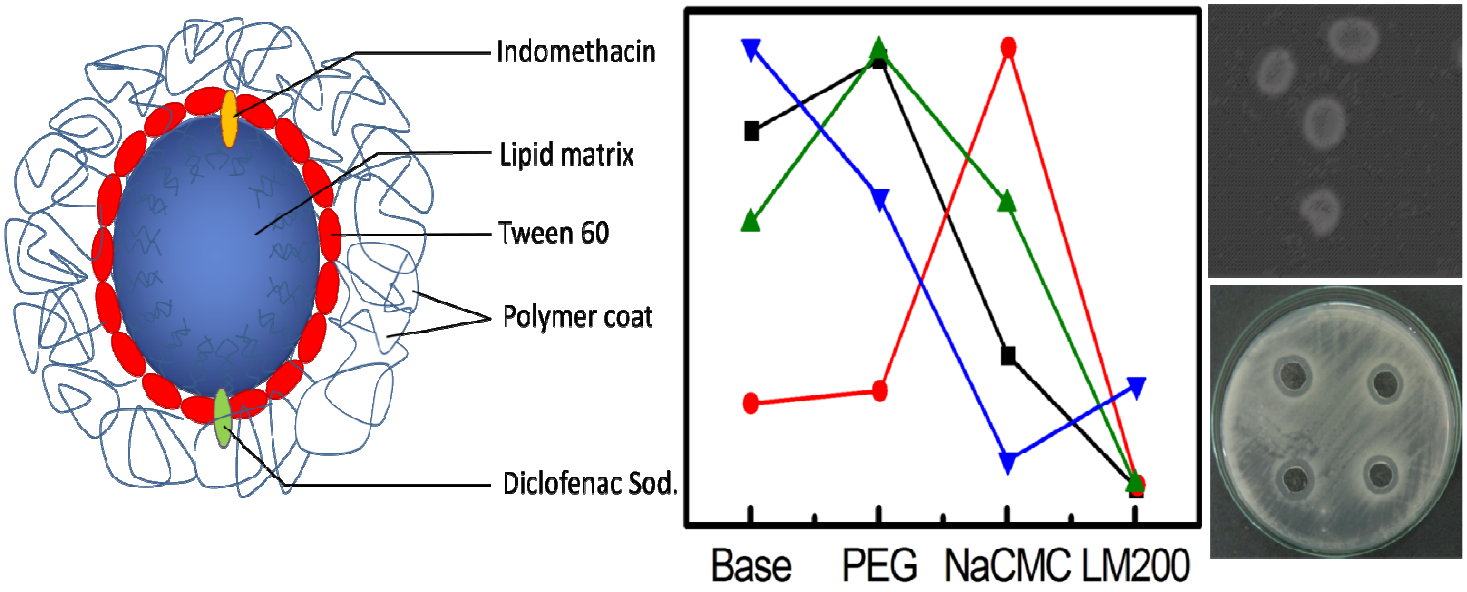

Proposed model of NSAID loaded and polymer coated NLC alongwith its dependence of size (■), PDI (●), release rate (▲) and absorption maxima (▼) as well as its morphology and antibacterial activity

RSC Advances

RSCPublishing

ARTICLE

Effect of Polymer Charge on the Formation and Stability of Anti-inflammatory Drug Loaded Nanostructured Lipid Carriers: Physicochemical Approach

Cite this: DOI: 10.1039/x0xx00000x

Received 00th January 2012,
Accepted 00th January 2012

DOI: 10.1039/x0xx00000x

www.rsc.org

Manish Sapkota,[1] Gourab Karmakar,[2] Prasant Nahak,[2] Pritam Guha,[2] Biplab Roy,[2] Suraj Koirala,[1] Priyam Chettri,[3] Kalipada Das,[4] Takeshi Misono,[5] Kanjiro Torigoe,[5] Amiya Kumar Panda[2,*]

Nanostructured lipid carriers (NLCs), with potential drug delivery capabilities, were formulated using soylecthin (SLC), tristearin (TS) and palmitic acid (PA) in the absence and the presence of two anti-inflammatory drugs, diclofenac sodium (DNa) and indomethacin (IMC). Tween 60 was used as stabilizer separetely in combination with sodium carboxymethyl cellulose (NaCMC, anionic), polyethylene glycol (PEG, nonionic) and N, N, dimethyl-N-dodecyl derivative of hydroxyethyl cellulose (LM200, cationic). Both DNa and IMC substantially decreased size and increased polydispersity index (PDI) of the NLCs. Hydrodynamic parameter, *viz.*, size, zeta potential and polydispersity index as well as the thermal behaviour of the NLCs depended on the type and charge of the added polymers. Weak interactions between drug and lipid matrices in the bulk mixtures were established through FT-IR studies. NLC formulations exhibited lower entrapment efficiency and loading content in case of DNa compared to IMC due to the higher ionic nature of the former drug. Polymers influenced the entrapment efficiency and loading ability of the NLCs in case of both DNa and IMC. 85% of the entrapped DNa was released from the NLC, compared to 54% release in case of IMC; the drug release rate were higher for PEG and NaCMC coated systems. LM200 delayed the drug release process with respect to NaCMC and PEG. Both DNa and IMC loaded NLCs inhibited the growth of gram positive bacteria, *Bacillus amyloliquefaciens*. It was concluded that the physicochemical properties of NLCs could effectively be modified by using polymers; thus the biomimetic characteristics of lipids and architectural advantage of polymers can be combined to yield a superior drug delivery system.

1. Introduction

Colloidal drug delivery systems have great potentials for their capability to decipher the issues related to pharmacokinetic and pharmacodynamic profiles of a large number of therapeutic agents. Such systems include microemulsion, micelle, nanosuspension, polymeric nanoparticle and liposome, *etc*.[1] Another classic group of drug delivery systemts include the liquid crystalline aggregates, more commonly known as cubosomes[2-12] and hexosomes.[13-15] While the cubosomes are discrete, nanostrucutred particles with bicontinuous liquid crystalline phases, hexosomes are aqueous dispersions of inverted type hexagonal phase.[16-18] Cubosomes are attractive vehicles for loading and delivering different drugs.[11] Solid lipid nanoparticles (SLNs) and nanostructured lipid carriers (NLCs) combine the advantages like targeted drug delivery, biocompatibility and sustained release, *etc*.[19] Besides, they can surmount toxicity, poor loading and stability issues related to drugs, as experienced by other colloidal systems.[19] Solid lipid nanoparticles (SLN) are aqueous colloidal dispersions of physiologically tolerated lipid components (solid at both physiological and room temperature) stabilized by emulsifiers.[20] Shortcomings of the SLNs include poor drug loading and expulsion during storage. In order to dispel the limitations, NLCs were introduced in late 1990s. NLCs are modified SLNs, where the highly ordered solid lipid matrices are replaced by spatially incompatible lipid blends with an aim to introduce more internal defects.[21] NLCs, therefore, can have improved performances compared to other colloidal carriers for which they are widely being explored.[19] Although NLCs are one of the most efficient available carrier systems, however, its major drawbacks include poor incorporation of hydrophilic molecules, higher lipid modification and aggregation due to the presence of spatially incompatible lipids, thus hindering their market availability.

Utility of nanocolloidal drug delivery system largely depends on its physicochemical stability and *in vivo* performance. Much interests have recently been focused on developing polymer stabilized nanoparticles providing core/shell architecture to improve

the stability and its surface chemistry.[22] Polymeric stabilizers, alone or in combination with surfactants, have been attached via physisorption or chemisorption on the surface of metal nanoparticles,[22] liposomes,[23] SLN[24] and even NLCs[25] in order to improve structural stability, drug delivery capability and biocompatibility, *etc*. Enhanced stability, induced by added polymers, largely depends on its structural and electrical properties, concentration and thickness of the adsorbed layer.[26] Furthermore, polymer charge can influence the stability of NLCs. Nonionic polymers (*e.g.*, polyethylene glycol, poloxamers, polyvinyl alcohol, *etc.*) sterically stabilize the NLCS.[27] On the other hand, polyelectrolytes can interact electrostatically to provide electrostatic stabilization in addition to the steric stabilization. The electrostatic stabilization involves repulsive interaction between particles carrying similar charge.[23, 28, 29]

In spite of its projected manifold applications, reports on polymer stabilized NLCs are scanty; large number of reports available in the literature are focused on the *in vivo* stabilization and surface functionalization.[22] Furthermore, no systematic studies have been made to compare the effect of charge and concentration of different polymers on the formation and stability of NLCs to the best of our knowledge. Thus studies on the effect of polymers, *viz.*, nonionic (polyethylene glycol-2000, PEG), anionic (sodium carboxymethyl cellulose, NaCMC) and cationic (hydrophobically modified cationic derivative of hydroxyethyl cellulose, LM200) separately in combination with a nonionic surfactant Tween 60 were considered to be significant. Both PEG and NaCMC are of GRAS status and have widespread uses in biomaterials and have been approved by FDA as excipients (FDA Inactive Ingredients Database) for use in the pharmaceutical formulations, cosmetics and food grade products.[30] They have also been extensively explored for their potentials in the formulation and stabilization of other nanoparticles. LM200, similar to NaCMC, is a modified cellulose derivative and has been widely used in hair care products.[31] However, little work has been done with this biocompatible cationic polysaccharide in the nanoparticle based drug delivery systems.

Diclofenac sodium (DNa, [2-[(2,6-dichlorophenyl) amino] phenyl] acetate, sodium salt) and indomethacin (IMC, 1-(*p*-chlorobenzoyl)-5-methoxy-2-methyl-3-indolylacetic acid), are the nonsteroidal anti-inflammatory drugs, most widely used in the treatment of acute and chronic inflammation as well as different types of pains.[32] They have also been explored for their anti-proliferative effects on tumor cells and anti-bacterial activities.[33] However, they share common side effects, *viz*., gastrointestinal (GI) ulcer, renal damage and impaired platelet function[34]. In order to minimize the side effects, studies on these two drugs in terms of their compatibility in surface modified NLCs are considered to be significant.

In the present work, surfactant-polymer stabilized NLC formulations were prepared with a blend of soylecithin (SLC), tristearin (TS) and palmitic acid (PA). Effect of polymer (PEG, NaCMC and LM200) charge and concentration on the physicochemical properties of NLCs were explored. Apart from the nature of carrier, inherent property of the bound drug can also affect the carrier; thus two drugs, DNa and IMC were used whereby their effects on the NLCs were studied. All the systems were characterized by analyzing their size, polydispersity index (PDI) and zeta potential (through dynamic light scattering), morphology (electron microscopy) and thermal (differential scanning calorimetry) analyses. Systems were further exploited to study its drug encapsulation efficiency, release profile and activity against gram positive bacteria (*Bacillus amyloliquefaciens*). It is believed that such comprehensive set of studies can explore the suitability of different polymers to effectively modify the physicochemical properties of anti-inflmmatory drug loaded NLCs.

2. Experimental section

2.1 Materials

The following chemicals were purchased: glyceryltristearate (tristearin, TS, Sigma-Aldrich, USA), soylecithin (SLC, Calbiochem, Germany), Palmitic acid (PA) and polyoxyethylenesorbitanmonostearate (Tween 60, Sisco Research Laboratory, India); sodium carboxy methyl cellulose (NaCMC, Merck Limited, Mumbai, India), polyethylene glycol-2000 (PEG, Alfa Aesar, Lancester, U.K). N,N-dimethyl-N-dodecyl derivative of hydroxyethyl cellulose (LM200) was a generous gift from the Centre for Surface Science, Dept. of Chemistry, Jadavpur University, Kolkata, India. Indomethacin (IMC) and diclofenac sodium (DNa) were kindly provided by Florid Laboratories Pvt. Ltd, Nepal and Torrent Pharmaceuticals, Sikkim, India respectively. All the chemicals used were stated to be ≥99% pure and were used as received. HPLC grade solvents and double distilled water with a specific conductance of 2 - 4 μS were used in preparing the solutions.

2.2 Preparation of NLCs

NLCs were prepared by hot homogenization followed by ultrasonication method.[35] Required amount of lipids (TS, SLC and PA) were dissolved in chloroform-methanol mixture (3:1, v/v); solvent was removed using a rotatory evaporator. The thin film thus obtained was melted at 75 °C followed by the addition of hot aqueous Tween 60 solution maintained at the same temperature. The coarse emulsion was exposed to high speed dispersion for 1 h; the obtained pre-emulsion was further processed with a probe sonicator (Takashi U250, Takashi Electric, Japan) at 150 W/(20-25) kHz maintaining the same temperature for a period of 1h to produce nanoemulsions, which were allowed to cool down at room temperature and stored at 4 °C to obtain NLCs.

Total lipid concentration in the dispersion was maintained at 1 mM in a molar ratio of SLC: TS: PA, 2:2:1. 10 mM Tween 60 was used alone or in combination with the polymers as stabilizer. Formulations were either prepared as drug free or loaded (0.1, 0.2 and 0.3 mM). All the polymers were initially mixed with surfactant solution and then added to the formulation whereas the drugs used were initially dissolved in chloroform+methanol system along with the lipids.

2.3 Characterization of the prepared NLCs

Hydrodynamic diameter (d_h), zeta potential (Z.P.) and polydispersity index (PDI) values were measured by a dynamic light scattering spectrometer (Nano ZS 90, Malvern, UK). Scanning electron

microscope (FEI Quanta-200 MK2, Oregon, USA) and freeze fractured transmission electron microscope (H-7650, Hitachi Science Systems Ltd., Japan) were used for the morphological investigations. Interaction between the drugs and lipid matrices were studied by means of FT-IR spectrometer (Spectrum RX I, Perkin Elmer Inc, USA). All the thermal analyses were performed using DSC 1 STAR^e system (Mettler Toledo, Switzerland). Absorption spectra of the drugs in solvents of different polarity and in NLCs were recorded using a UV-vis spectrophotometer (UVD-2950, Labomed Inc., USA).

2.4 Drug entrapment efficiency and loading capacity studies

Drug entrapment efficiency and loading content was determined by ultracentrifugation method. The resulting drug loaded NLC formulations were centrifuged at 10,000 rpm for 30 min maintained at a temperature of 4 °C such that the NLC-bound drug got sedimented leaving unbound one in the supernatant. The amount of free drug in the supernatant was estimated colorimetrically. Entrapment efficiency (EE) and drug loading capacity (DL) of NLCs were estimated using the mentioned equations:[36]

$$EE = \frac{W_a - W_s}{W_a} X\ 100 \quad (1)$$

$$DL = \frac{W_a - W_s}{W_a - W_s + W_L} X\ 100 \quad (2)$$

where, W_a, W_s and W_L are the weight of total drug, free drug in the supernatant and total lipid respectively.

2.5 *In vitro* drug release and release kinetic studies

In vitro release kinetics of the drug loaded in NLCs were evaluated using the standard dialysis bag method with 10 mM of Tween 60 as the release medium as described elsewhere.[37] Released drugs were quantified colorimetrically at 276 nm and 320 nm for DNa and IMC respectively. Data obtained from the *in vitro* release studies were fitted to Higuchi, Korsmeyer-Peppas and Weibull release kinetic models, the equation for each model has been represented as:[38]

Higuchi model: $$M_t = k_h t^{1/2} \quad (3)$$

Korsmeyer–Peppas model: $$M_t/M_\infty = k_k t^n \quad (4)$$

Weibull model: $$M_t/M_\infty = 1 - \exp\left[\frac{-(t-T_i)^\beta}{a}\right] \quad (5)$$

where, M_t is the amount of drug released in time (t), M_t / M_∞ is the fraction of drug released, 'n' is the release exponent that characterizes the mechanism of drug release, k_h and k_k are release constants for Higuchi and Korsmeyer–Peppas equation respectively, t accounts for the time lag of the dissolution process. 'a' denotes a scale parameter that describes the time dependence; β describes the shape of the dissolution curve progression.

2.6 Anti-bacterial susceptibility test

The cup-plate method[39] was adopted to study the antibacterial activity of both IMC and DNa loaded NLCs. The studies were carried out using two gram positive bacteria: *Bacillus amyloliquefaciens* and *Bacillus subtilis* and two gram negative bacteria: *Pseudomonas putida*and *Klebsiella pneumonia* respectively. Nutrient broth and agar were used as culture media and solidifying agent. In the pre-incubated plates, bacterial suspension (0.1 mL of 5×10^5 CFU mL^{-1}) was homogeneously spread over the agar surface and then grooves of equal diameter (0.7 cm) were made. In the grooves, 100 µL NLCs were added. The plates were incubated at 37 °C for 24 h. Antibacterial activity was quantified by calculating the zone of inhibition.

3. Results and discussion

3.1. Dynamic light scattering studies

Size and its distribution of NLCs are considered to be the markers of its physical stability during long-term storage.[19, 40] DLS technique was used to determine the particle size and PDI value of all the NLC formulations during a storage period of 90 days at 4 °C. Representative size distribution curves have been shown in Fig. 1. Sizes of the NLCs ranged from 150 to 400 nm with unimodal distribution.

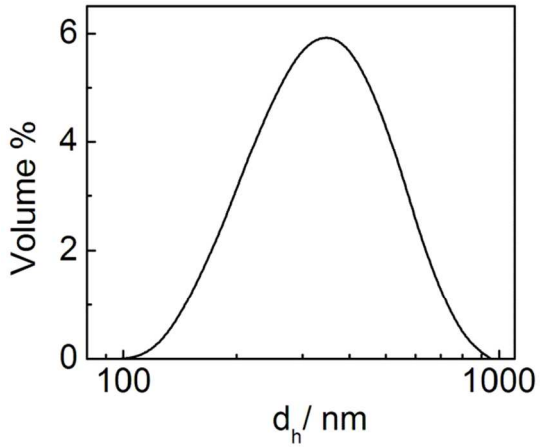

Fig.1 Size distribution curve for the NLC (SLC+TS+PA, 2:2:1 M/M/M, 1 mM) dispersed in aqueous Tween 60 (10 mM) medium at 25 °C.

Effect of the charge and concentration of polymer as well as the drugs on the size variation of the different NLC formulations with time have graphically been represented in Fig.2, Fig.S1 and S2 (supplementary section) respectively. The fluctuation in the hydrodynamic diameter was observed upto 10-15 days from the initial day of preparation which could be rationalized on the basis of the lipidic reorganization inside the NLC matrix. NLCs are prepared by using structurally different lipidic components. Due to dissimilarity and chain mismatch, structural reorganization among the lipidic components inside the NLC matrix is a very common phenomenon.[41,42] Reorganization of the lipid molecules in the NLC matrix makes the core mobile and leads to the fluctuation in hydrodynamic diameter of the NLCs during storage time. It is also possible that there is more than one population of the nanoparticles in addition to the micelles formed in the presence of the nonionic stabilizer Tween 60. This rearrangement of the component generally

takes 10-15 days from the day of preparation in our experiments as evident from size fluctuation in NLCs for almost 15 days. However, stable dispersion was obtained after 15 days which is confirmed by uniform size *vs.* time profile in most of the cases. Subsequently, all the dispersions were found to be stable up to a period of 90 days.

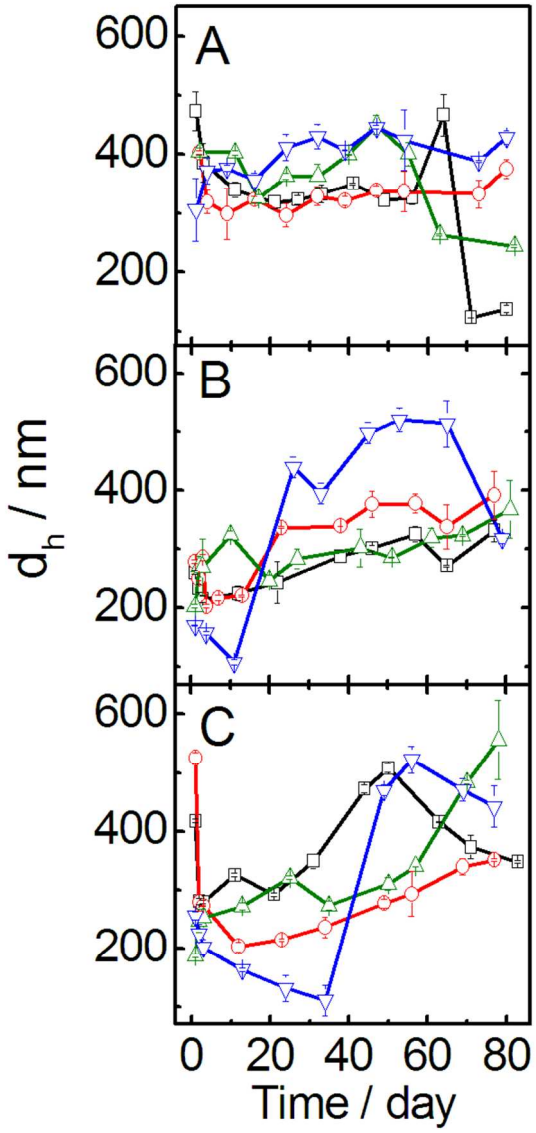

Fig.2 Variation in the hydrodynamic diameter (d_h) of NLCs (SLC+TS+PA, 2:2:1 M/M/M, 1 mM) dispersed in aqueous surfactant - polymer media (10 mM Tween 60+0.01 wt% polymer) at 25 °C. Panel A: d_h – time profile of drug free NLC; panel B: 0.2 mM DNa loaded NLC and panel C: 0.2 mM IMC loaded NLC.Systems: □, base NLC; ○, PEG-coated; Δ, NaCMC coated and ▽, LM200 coated NLC respectively.

PEG coated systems were found to be smaller than the base-NLCs as also reported by others.[43, 44] Because of its hydrophilicity PEG, along with Tween 60, allows rapid emulsification of oily phase by providing W/O interfaces which supports the formation of smaller particles. However, increase in size with increasing PEG concentration was due to the availability of PEG molecules to result in the expansion of interface.[44] Due to similarity in the charges, poor film formation and non-uniform mass uptake led to large variation in size in case of NaCMC stabilized systems.[45] Systems stabilized by LM200 were bigger than the other two polymers as well as the base system; increase in size was concentration dependent, as observed by other research groups.[46] Electrostatic attraction between the cationic polymer and the anionic NLCs could lead to the deposition of the polymer on the surface of the NLC. Minimum variation in size and its distribution were experienced in the presence of 0.01 wt% polymer irrespective of their charges. Further studies, therefore, were carried out at this particular polymer concentration. Incorporation of DNa and IMC in NLC resulted marked effects on particle size and the PDI values. Both the drug loaded systems showed similar trend compared to drug free systems; reduction in size and increase in PDI value with increasing drug concentration, like others.[47]

Decrease in size for the base-NLC loaded with DNa was more prominent than IMC loaded systems, which showed almost similar trend like the base-NLC. Both the drugs being amphiphilic, can be adsorbed on the NLCs. DNa being completely ionized, interacts at the interface and dehydrates the phospholipid or the ethylene oxide head group of the nonionic surfactant and thus reduction in the interfacial hydrodynamic curvature was observed.[48, 49] Due to its lesser ionic nature, deeper penetration of IMC into the lipid surface during the solidification of lipid melt would prevent its interaction with the polar head groups to minimize the surface effect as observed for DNa. Increase in size with time for IMC loaded base-NLC was due to the agglomeration of lipid matrix induced by the drug. IMC got excluded from the surface of NLC because of its increased hydrophilicity in the presence of PEG. Similar effect was observed for drug loaded NaCMC coated systems.[50] LM200 caused significant size decrease for both the drugs which was due to the decrease in attractive electrostatic attraction between cationic polymer and lipid matrix in presence of the anionic drug.[51] However, absence of any precipitate was due to adsolubilisation of the dissociated components into the bulk, aided by the surfactant present in the medium. Progressive decrease in size supports the existence of hydrophobic interaction in addition to electrostatic interaction between the polymer and lipid matrix. Nevertheless, a marked increase in size with time is related to the instability of the system, *i.e.*, the formation of precipitates with time.

Variation in polydispersity index (PDI) with time for all the systems has been represented in Fig. S1, S3 and S4 (supplementary section). Higher PDI values indicate the formation of differently sized particles. The free or unbound Tween 60 that forms micelles like entity with an average diameter of 8-10 nm (data not shown) and the increased mobility of the internal lipids and fluidity of the surfactant layer due to the presence of higher concentration of unsaturated soylecithin[52] may account for the increased PDI. Further increase in PDI with time was due to the aggregation of the NLCs. Marked increase in PDI values with time in the presence of both the drugs (Fig. S1 and S4, supplementary section) suggest its destabilization effect on the NLCs.

Zeta potential (Z. P.) of some representative formulations are shown in Fig. 3; results for all the other systems have been shown in the supplementary section (Fig.S5 and S6). Z. P. of the blank NLC was -11 mV in the begining (day 1 of sample preparation). Negative zeta potential of the formulations could be rationalized by the presence of dissociated fatty acids. Palmitic acid was used as one of

the lipidic components of NLCs. Palmitic acid may undergo dissociation/ ionisation thereby enhancing the magnitude of the negative zeta potential. Fatty acids are very important component for NLCs because they are found to stabilize the lipid dispersion by enhancing the zeta potential value (through the dissociation of carboxylic head group). Observed lower magnitude of Z.P. indicates significant adsorption of the nonionic surfactant over the NLC surface which also provides good steric stabilization to the colloidal dispersion.[40, 53]

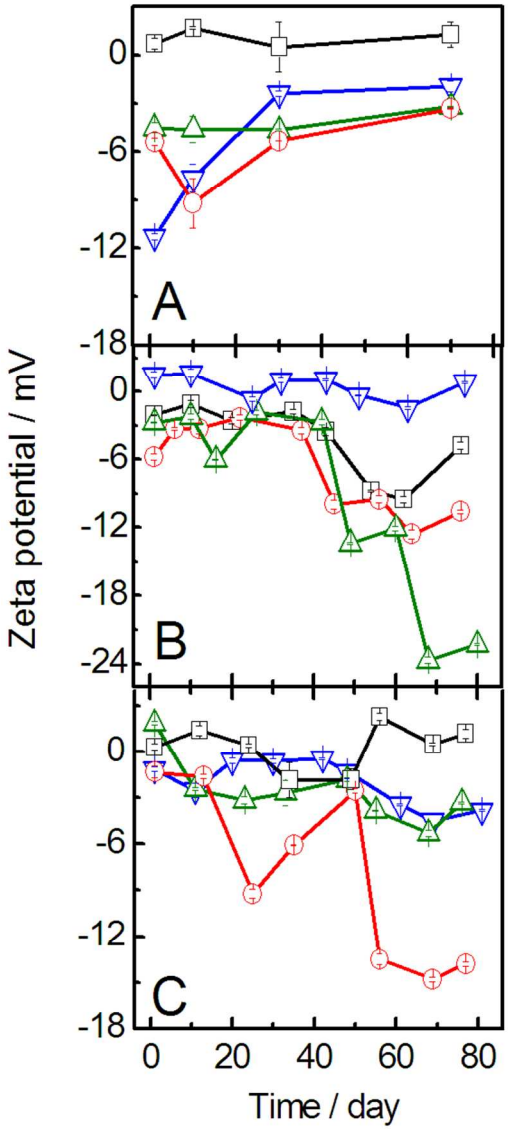

Fig.3 Variation of the zeta potential of NLC in the absence and presence of non-steroidal anti inflamatory drugs with time at 25 °C. SLC+TS+PA, 2:2:1 M/M/M, 1mM dispersed in aqueous surfactant - polymer media (10 mM Tween 60+0.01 wt% polymer) were used. Panel A: drug free NLC; panel B: 0.2 mM DNa loaded NLC and panel C: 0.2 mM IMC loaded NLC. Polymers: □, base (no polymer); ○, PEG; Δ, NaCMC and▽, LM200.

Magnitude of negative Z.P. further decreased (-4 mV) upon the addition of PEG; which was due to the shielding of charges by PEG, inherent property of this nonionic hydrophilic polymer.[43] Such an observation also further supports the size reduction in the presence of PEG. Although the magnitude of Z.P. was reduced for PEG-NLC systems, the value increased with increasing PEG concentration. NaCMC-stabilized systems represent almost similar behaviour like the blank systems; however the magnitude Z.P. was higher than the blank suggesting probable adsorption of NaCMC on the NLC surface. Electrostatic interaction and the adsorption of LM200 over the NLC surface is evident from the reduction in the magnitude of the negative zeta potential upon increasing polymer concentration.[54] Magnitude of negative Z.P. for the blank and NaCMC-stabilized systems decreased with time when analyzed for a period of 80 days whereas the change was negligible for PEG and LM200. Results indicate the desorption of the anionic polymer from the NLC surface; on the contrary, nonionic and cationic polymers provide better stability to the NLC due to their lesser desorption probability. Z.P. for the drug loaded systems were also compared with drug free systems, as shown in Fig. 3. Incorporation of the drugs did not significantly alter the surface charge densities of PEG and LM200 stabilized NLCs. Initial decrease in Z.P. values for both the drug loaded base and NaCMC-stabilized systems were observed which was due to the compression of the electrical double layer by the electrolytes upon the addition of weakly acidic drugs.[55, 56] Increase in negative zeta potential was observed after 40 days for both the drugs except LM200.[57] The negatively charged NLC surface promoted the expulsion of the drugs.

3.2 Morphological studies

Shape and surface morphology of base NLC, assessed after 20 days of preparation by scanning electron microscopy (SEM) and freeze fractured transmission electron microscopy (FF-TEM). Some representative images have been shown in Fig. 4 and Fig.5 respectively.

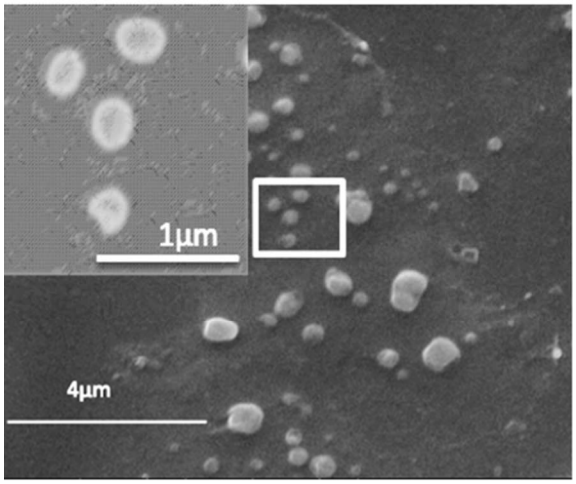

Fig. 4 Scanning electron micrograph of 0.2 mM DNa loaded NLC (SLC+TS+PA, 2:2:1) dispersed in aqueous Tween 60. Scale bars are mentioned in the images.

Discrete, smooth and spherical shaped morphologies were noted. Results were more or less similar for the other formulations. Incorporation of drugs were found to show no characteristic amendment in the morphology of the NLCs. Some agglomerates were found due to the drying process during sample preparation. The average particle size of NLCs calculated from SEM as well as FF-TEM studies ranged between 250-300 nm, which were smaller than the same as obtained by DLS studies.

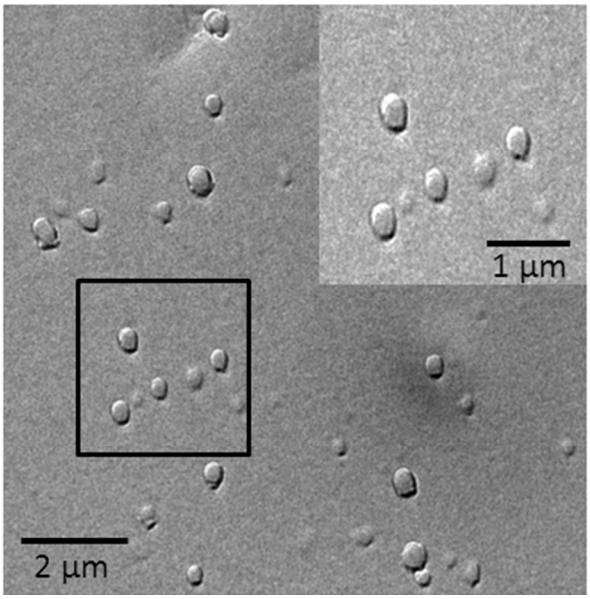

Fig. 5 Freeze fractured electron micrograph (FF-TEM) of 0.2 mM NLC (SLC+TS+PA, 2:2:1) dispersed in aqueous Tween 60. Scale bars are mentioned in the images.

The discrepancy in particle size is due to the difference in the measurement principles involved. DLS measures the hydrodynamic diameter in the solution phase whereas the electron microscopic measurements are carried out at complete dry condition which would lead to the little shrinkage of the radius of hydration and present particles with smaller size as compared to DLS.[58] Electron microscopic (EM) techniques can easily provide accurate size measurements with sub-nanometer resolution. However, organic surface ligands are difficult to resolve owing to their low electron density, so the EM determined size mainly reflects the size of the core. In addition, the requirement of high vacuum for EM imaging calls for complicated sample preparation procedures that can result in nanoparticle aggregation.

3.3 FT-IR studies

FT-IR studies are useful in understanding the interaction between drug and lipidic components which, to a large extent, determines the physicochemical properties of the prepared lipid formulation. FT-IR spectra for pure drug and physical mixture of lipid matrix alone or in the presence of drugs (IMC and DNa) were obtained and analyzed in the region of symmetric and antisymmetric vibration of -CH_2- group, carbonyl stretching region and phosphate group frequency region (Fig. S7). The lipid mixture exhibited characteristic band for O-H (stretch) at 3394 cm^{-1}, methylene asymmetric and symmetric stretching at 2917, 2956 (shoulder) and 2850 cm^{-1} respectively; carbonyl (C=O) band at 1736 cm^{-1}, wagging and twisting mode of CH_2 was marked by the presence of large number of bands between 1196-1302 cm^{-1}, C=O stretch at 1180 cm^{-1}, rocking mode of CH_2 at 717 cm^{-1}.[59-61]Na shows the band characteristic of secondary amine groups (3388 cm^{-1}), phenyl groups (1577 cm^{-1}) and substituted phenyl group stretch (748 cm^{-1}).[62] On the other hand, IMC has bands characteristic of basically two carboxylic groups as observed at 1692 cm^{-1} for benzoyl vibration and at 1717 cm^{-1} for acid carbonyl stretching. These peaks are characteristic peaks for γ form of IMC because of the presence of the anhydride groups formed as a consequence of the interaction of the acidic hydrogen with the amide-carbonyl group of a second molecule. When lipids are separately mixed with DNa and IMC, a marked broadening of the peaks at 2917 and 2850 cm^{-1}, assigned for methylene asymmetric and symmetric stretching respectively, were observed. These peaks are highly sensitive to the variation in intermolecular chain–chain interaction and can be taken as a probe for lipid order and packing.[60] Broadening of the bands suggests that both the drugs, being weak acids, are less ionized at this condition which can penetrate deeper into the NLC and thus are capable to interact with the acyl chain within the core leading to the increase in mobility of lipid matrix. This is further supported by the absence of any shift of the peaks of the phosphate group (1220-1260) cm^{-1} of phospholipids.[63] The carbonyl group vibration comprised two bands: one at 1736 cm^{-1} (non-hydrogen bonded) and 1728 cm^{-1} (hydrogen bonded). Carbonyl bonds are highly sensitive to hydrogen bonding and conformational effects.[63] Upon incorporation of the drugs into the physical mixture, increase in the high frequency band with a broader peak in the frequency region of 1738-1740 cm^{-1} was observed, which was due to the dehydration of the carbonyl moiety upon interaction with DNa and IMC.[63]

3.4 Differential scanning calorimetry (DSC) studies

DSC curves for bulk lipid mixture and the NLC formulations in the absence and presence of the drugs as well as the polymers are shown in Fig. 6 and Fig. 7. A marked reduction in the temperature of

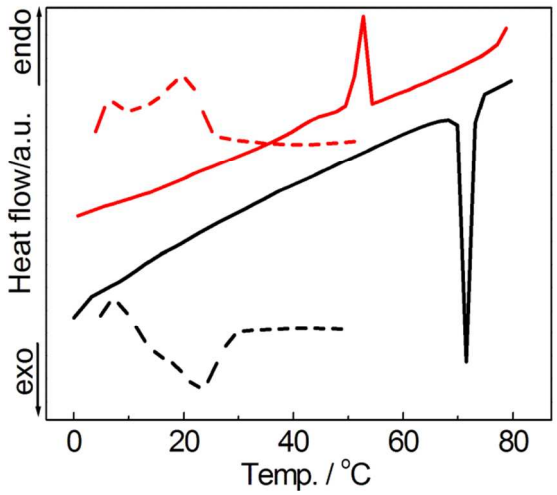

Fig.6 DSC thermogram of the physical mixture of lipid and base-NLC (SLC+TS+PA, 2:2:1 M/M/M, 5 mM dispersed in Tween 60, 10 mM).- - - -, heating curve of base-NLC; - - - -, cooling curve base-NLC; ▬, heating curve of the physical mixture and (▬), cooling curve of the physical mixture. Scan rate: 2 °C/min.

maximum heat flow (T_m, in the range of 19 – 20.5 °C) with the broadening in the thermograms were noted compared to the bulk physical mixture of the lipids (52 °C). Reduction in the T_m value was due to structural reorganization and subsequent generation of imperfections induced by Tween 60. According to Thomson proposition,[56] decrease in T_m values is due to the decrease in size.

Appearance of both the exo- and endothermic peaks excludes the existence of supercooled entities. The heating endotherm appeared in the temperature range of 23-25 °C while the cooling exotherms were downshifted (19.3 - 20.4 °C) as also observed by others.[64] The exothermic peaks were further analyzed because of its distinctness compared to the heating curves.

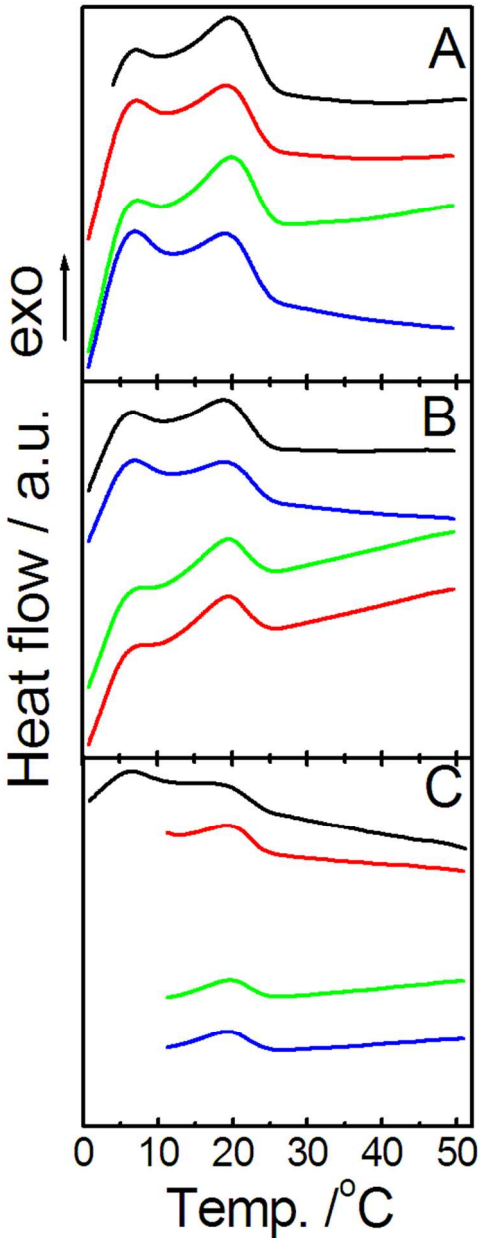

Fig.7 DSC cooling thermograms of drug free and drug loaded NLCs. A, drug free; B, DNa loaded and C, IMC loaded. Systems for all the panel: —, base-NLC —, PEG; —, NaCMC and —, LM200-stabilized NLC respectivly. Concentrations of NLCs: 5 mM, polymer: 0.05 wt% and drug: 1 mM. Temperature range 0-80 °C and scan rate: 2 °C/min.

Derived thermodynamic parameters of the DSC studies, *viz.,* temperature of maximum heat flow (T_m), peak width (ΔT), changes in enthalpy (ΔH), heat capacity (ΔC_P) and crystallinity index (CI) have been summarized in Table 1. T_m values passed through minima for 0.05 wt.% added polymers. Shift in the T_m values were in the range of 0.1 to 0.5 °C for different amount of added polymers; such Observations were indicative of insignificant interactions between the polymer and the lipid core. However, small increase in the peak intensity with increasing polymer concentration was due to its shielding effect. Significant interaction between the lipid matrices and the drugs could be established through the reduced T_m values upon the addition of drugs. Polymers significantly decreased the ΔH values of the NLC (76.03 kcal mol^{-1}) which was due to the creation of lattice defects induced by the added polymer. Changes in the ΔH values of the NLCs were dependent on the type of polymer. In the lower concentration range, PEG significantly lowered the ΔH values. Results could be rationalized on the basis of marked decrease in size and crystallinity of the NLCs by PEG. In the higher PEG concentration region, increase in ΔH value could be explained on the basis of increased size of the NLCs. Unlike PEG, ΔH values continuously decreased with increasing LM200 concentration (from 51.44 to 48.62 kcal mol^{-1}). Increased size with added LM200 resulted such kind of observations. Besides, electrostatic attraction between NLC and LM200 resulted in the formation of more organized structures. For NaCMC-stabilized systems, ΔH value passed through minimum with increasing polymer concentration, however, in a nonsystematic way. Combined DSC results thus suggest that the effect of polymers were significant at lower concentration; but the effect became insignificant in the higher polymer concentration range. Both the drugs suppressed the ΔH values; the effect was more prominent in case of IMC for its lower polarity and subsequent better insertion capability into the lipid matrices.

Width of the chain melting peak is a marker of the extent of crystallinity of the NLCs. Broadening of peak with added polymer is an indication for the probable formation of ultra-thin polymer layers of the NLCs. Observation could further be correlated with the observed change in ΔC_p values, which decreased with increasing polymer concentration. Extent of the depletion in the ΔC_p values followed the order: LM200 > PEG >NaCMC, which were in accordance with the extent of electrostatic attraction between NLC and the polymers. Increase in peak width was higher for IMC than DNa for obvious reason: polarity of the drugs. Furthermore, in an attempt to confirm the interaction of polymers as well as the drugs with NLCs, crystallinity index (CI) of the studied formulations were determined by considering the base NLC as the pure component (with 100% CI). Involvement of the polymers was clearly indicated by the reduced CI in all the cases. In addition, the reduction in CI value for the drug loaded formulations provided additional information regarding drug interaction with NLC. Reduction in CI values was significant for the drug incorporated systems. The results could be considered as signature of the interaction between the drug and NLC whereas the polymers only forms coat/layer surrounding the NLC, accompanied by Tween 60. The obtained results were further confirmed by the FT-IR as well as spectrophotometric investigations in the latter sections. However, to bit the final nail on this issue, further experiments like small and wide angle X-ray scattering (SAXS and WAXS) methods may be carried out which would provide important information on the effects of lipid composition, polymer type and penetration of drug on the crystalline structure.[4, 65] These are considered to be the future perspectives of the present set of works.

Table 1. DSC data of different NLC formulations in the presence of drug and polymer.

Polymer	Wt% of polymer	T_m/ °C	ΔT/ °C	ΔH/k cal. mol^{-1}	ΔCp/k cal/ mol/°C	%CI
NLC-base	-	19.98	6.36	76.03	11.95	100
NLC-PEG-2000	0.001	19.76	5.40	54.32	10.06	71.4
	0.01	19.77	6.08	57.23	9.41	75.2
	0.1	19.88	6.58	59.42	9.03	78.1
NLC-NaCMC	0.001	19.31	5.06	54.98	10.87	72.3
	0.01	20.13	7.25	74.36	10.26	97.8
	0.1	20.43	6.98	72.84	10.44	95.8
NLC-LM200	0.001	19.54	5.57	51.44	9.24	67.6
	0.01	19.88	5.22	49.95	9.57	65.6
	0.1	20.01	6.08	48.62	8.00	63.9
Drug loaded systems coated with 0.01wt% polymer						
Drug	**Polymer**					
DNa	-	19.76	7.57	12.61	1.67	16.5
	PEG-2000	19.60	7.22	12.93	1.94	17.0
	NaCMC	19.32	7.80	14.30	1.66	18.8
	LM200	19.40	7.43	13.97	1.93	18.3
IMC	-	19.50	7.86	9.16	1.17	12.0
	PEG-2000	19.53	7.03	12.53	1.67	16.4
	NaCMC	20.07	6.32	11.32	1.98	14.8
	LM200	19.87	6.88	11.73	1.65	15.4

0.2 mM drug was used in each case. T_m, temperature for maximum heat flow; ΔT, peak width; ΔH, enthalpy change and ΔC_p, heat capacity change. 1 mM NLC (SLC+TS+PA, 2:2:1 M/M/M) was dispersed in aqueous surfactant - polymer media (10 mM Tween 60+polymers). Scan rate: 2 °C/min

3.5 Spectroscopic studies

State of polarity of the drugs were evaluated by comparing the UV-visible absorption spectra in NLCs with the same in solvents of different polarity. UV-visible absorption spectra of DNa and IMC in different solvents and in NLC are shown in Fig. 8. Dependence of absorption maxima (λ_{max}) on the dielectric constant of the medium are also shown in Fig. S8. Absorption maximum (λ_{max}) for DNa in NLCs was 281 nm, while in water it was at 276 nm. No such shift in the λ_{max}^{abs} (320 nm) was observed for IMC. Polarity of the drugs as established in NLCs, were found to be 19.79 and 20.1 for DNa and IMC respectively. Results suggest independence of the polarity effect of IMC. DNa being more ionic in nature, resides on the surface of the NLCs and are expected to be affected by the polarity of local environment. Similar shift in the absorption maximum of DNa to higher wavelength has been reported by Mehta *et al.*[66] Association of DNa with the polyoxyethylene moiety of Tweens

might have played a role in this regard. The drug molecules may get weakly intercalated on the surface of NLC. Thus, the microenvironment would be expected to be less polar resulting in a shift in λ_{max}^{abs} for DNa.

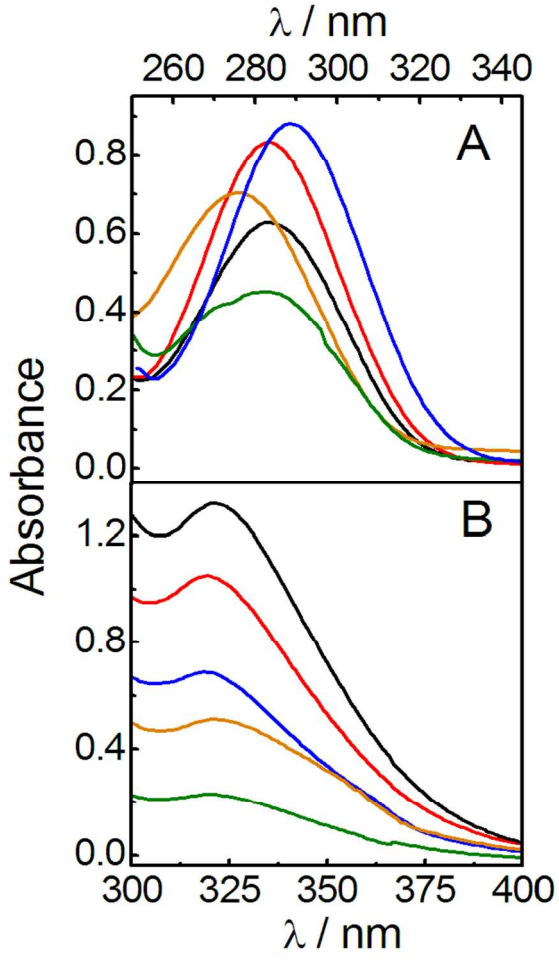

Fig.8 UV-visible absorption spectra of 0.2 mM DNa (A) and IMC (B) loaded in NLC as well as in different solvents at 25 °C. Solvents / systems : ——, chloroform; ——, ethanol; ——, DMSO; ——, water and ——, drug loaded NLC.

3.6 Drug entrapment efficiency and drug loading capacity studies

Entrapment efficiency (EE) and drug loading capacity (DL) of the surface modified NLCs were evaluated and the effect of polymer charge on the incorporation of both the drugs were also inspected. The obtained results have been summarized in Table 2. While considering the drug incorporation, systems were found to be similar to the lipid based lyotropic liquid crystal systems having cubic and hexagonal lamellar phases.[9, 13] Due to the hydrophilic nature of DNa, its physical exclusion from NLC is higher that resulted in its lower EE and DL. Solid lipids in combination with the liquid or unsaturated lipids are used in preparing NLC. In case of hot homogenization approach, high temperature sonication of the formulation results in a nano emulsion dispersion comprising all the lipid melts including the drug.

Table 2. Incorporation efficiency and loading capacity of NLC formulmation in the absence and presence of polymers for the drugs diclofenac sodium (DNa) and indomethacin (IMC)

Formulations	DNa		IMC	
	EE%	DL%	EE%	DL%
NLC- base	65.9±0.8	5.2±0.1	70.8±0.7	6.2±0.1
NLC-PEG2000	65.8±0.4	5.2±0.1	71.9±2.1	6.5±0.2
NLC-NaCMC	58.4±0.9	4.6±0.1	71.7±2.3	6.3±0.3
NLC-LM200	66.9±0.7	5.3±0.1	71.0±0.4	6.2±0.1

1 mM NLC (SLC+TS+PA, 2:2:1 M/M/M) was dispersed in aqueous surfactant-polymer media (10 mM Tween 60 + 0.01 wt% polymer). 0.2 mM drug was used in each case.

Upon cooling, nano droplets of the lipid melts start to solidify and form the NLC. This is known as the NLC hardening. During this hardening process, solubility of the incorporated drug in the lipid melt is reduced and some excess drug, especially the hydrophilic drugs, gets expelled from NLC. The drug expulsion due to the reduced drug solubility at the time of NLC hardening is known as physical exclusion phenomenon.[67] However, high lipid solubility of IMC prevents the physical exclusion phenomenon during NLC hardening that explains its higher EE as well as DL.[67] Charge of the polymers did not exhibit significant effect on the incorporation of IMC. IMC resides in the core of the NLC owing to its lipophilic nature and higher lipid solubility; thus, its interaction with the surface adsorbed polymer is improbable. In case of DNa, both EE and DL were remarkably influenced by the nature of polymer employed in the dispersion medium. The entrapment efficiency of DNa in base-NLC and PEG-NLC was almost similar. Minimum EE and DL was observed with NaCMC-NLC system which can be explained by the electrostatic repulsion between the negatively charged polymer and drug that leads to easier exclusion of the surface adsorbed negatively charged DNa. Formulation containing LM200 entrapped highest amount of DNa due to the tendency of positively charged LM200 to electrostatically bind the surface adsorbed DNa.[68]

3.7 *In vitro* drug release studies

Release profile of DNa and IMC from the NLCs have been shown in Fig. 9. NLCs markedly sustained the release of both the drugs; release profiles were dependent on the polymer. Maximum drug release of DNa from NLC was observed for PEG stabilized systems (85% after 96 h) and for IMC, both PEG and NaCMC stabilized systems showed maximum drug release profile (~50% after 96 h) whereas LM200 retarded the release of both the drugs. The drug loaded systems in absence of any polymer as well as PEG stabilized system showed intermediate behavior. Higher release for DNa was due to its greater hydrophilicity than IMC.[69] Higher release profile for PEG comprising system was due to the decreased polarity of the release medium induced by the polymer.[47] Sustained release of DNa from NaCMC stabilized system was comparatively less than the PEG which hints towards the formation of some drug loaded micelle

and enhanced viscosity of the system at low NaCMC concentration.[70] The cationic polymer showed a further retarded release profile (compared to the nonionic and anionic polymers), indicating probable electrostatic interaction between the drugs and polymer. LM200, being a hydrophobically modified polymer, has distinct $-C_{12}H_{25}$ hydrophobic residue alongwith cationic quaternary ammonium centres;[71] thus the hydrophobic nature of the polymer makes it less susceptible to hydration and may reduce the permeability of water into the nanoparticles which retards the release process.

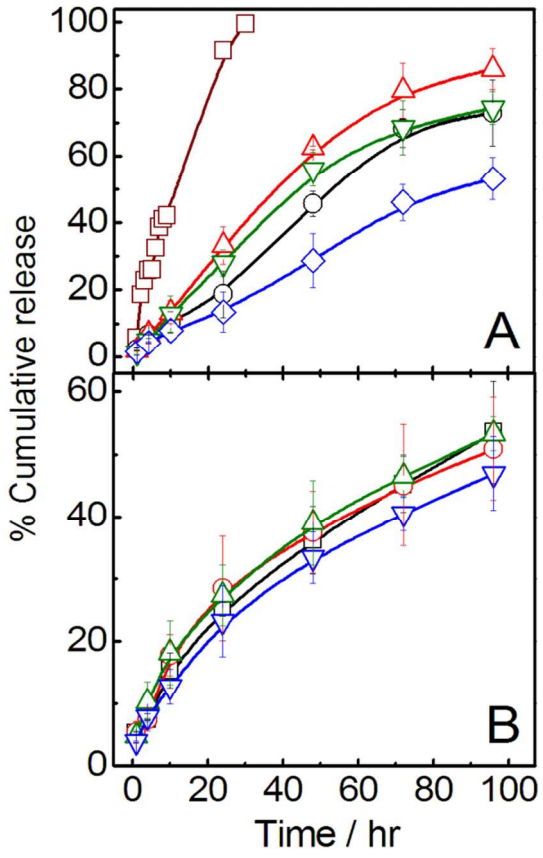

Fig.9 *In vitro* release profile of DNa (A) and IMC (B) from NLC (SLC+TS+PA, 2:2:1 M/M/M, 1 mM) matrices at 25 °C. 0.2 mMDNa and IMC were used. Systems: □ drug in Tween 60, ○, base-NLC; Δ, PEG; ▽, NaCMC and ◊, LM200 stabilized NLC. Each point was represented as mean ± (S.D.) (n=3).

In order to determine the suitable drug release kinetic model describing the dissolution profile, DDSolver 1.0, an Add-In Program for Modelling and Comparison of Drug Dissolution Profiles were used.[38] The obtained release data were fitted into Higuchi, Korsmeyer-Peppas and Weibull equation, as mentioned earlier (eq. 3-5). Rate constant value for the release process was calculated from the slope of the appropriate plots; the associated regression co-efficient (r^2) values were also evaluated, as shown in Table S1 (supplementary section). Release of drug from NLCs followed Weibull and Korsmeyer-Peppas equations better than the Higuchi equation. However, some differences in the release profile ofIMC and DNa were also noted. IMC release profile was better correlated to all the three models applied with only a minute variation whereas a higher degree of variation for DNa release profile was observed where the (r^2) value for Higuchi model did not fit well. Value of release exponent (n) which characterises the release mechanism as proposed by Korsmeyer and Peppas was observed to be less than 0.5 with minor variation for IMC loaded systems which suggests that the release of IMC from the lipid matrix was dominated by Fick diffusion whereas the (n) value for DNa loaded systems was observed to be (1>n>0.5) which suggests that the release of DNa from the NLCs was anamolous meaning non-Fickian diffusion behavior. It is proposed that as a result of contributions from diffusion and polymer erosion, *i.e.,* contributed by the combination of dissolution and diffusion can be correlated to the poor fit of DNa release profile to Higuchi model**.** The release rate constant obtained from Higuchi model has been tabulated and revealed that the release rate followed an ascending order: LM200 < PEG < NaCMC < base NLC, or no polymer for IMC loaded systems. For DNa loaded systems the following sequence was observed LM200 < base -NLC < NaCMC < PEG. Results are in accordance with the observed release profile. The shape parameter, β, obtained from Weibull model for the IMC loaded systems represented a parabolic curve, *i.e.*, case 3 whereas S-shaped curve was observed for DNa loaded systems with β value more than 1.

3.8 Anti-bacterial activity studies

Due to the increasing incidence of antibiotic resistance, different drugs apart from anti-microbial agents have been explored as possible alternatives and are referred to as non-antibiotics.[72] Anti-inflammatory drugs, apart from their anti-inflammatory effects, have also been explored for their anti-bacterial activities against both gram-positive and gram-negative bacteria. They are also reported to show synergistic effect when used in combination with antibiotics.[33] Thus in this study, the antibacterial activity of both DNa and IMC loaded NLCs against two different strains of each group, *i.e.*, gram positive and gram negative bacteria were explored. Initially, minimum inhibitory concentration (MIC) of both the drugs against the studied strains of bacteria was determined experimentally by varying concentrations of drug from 1-10 mM. The results as observed showed no zone of inhibition for both the drugs against gram negative bacteria whereas both DNa and IMC were found to inhibit the growth of gram positive bacteria (*Bacillus amyloliquefaciens*) at a minimum concentration of 0.2 mM. As the drugs did not inhibit the growth of gram negative bacteria, further studies with different NLCs loaded with DNa and IMC in a concentration of 0.4 mM were carried out only against the strains of gram positive bacteria considering drug free NLCs as control. All the drug loaded systems were found to show significant antibacterial activities. No antibacterial activity was found with the systems devoid of both the drugs. The obtained distinct zone of inhibition (24 h of incubation at 37 °C) for DNa and IMC loaded NLCs are shown in the Fig. 10.

The percentage zone of inhibition was calculated for all systems studied and was found to be independent of the type of polymer. DNa exhibited better anti-bacterial activity against both the strains than the IMC. 49-53.5% area was inhibited in all the cases. Obtained

results clearly concluded the potential antibacterial activity of DNa and IMC loaded NLCs. However, further studies using other bacterial strains are required to explore the broad spectrum antibacterial activity of NLCs loaded with these drugs.

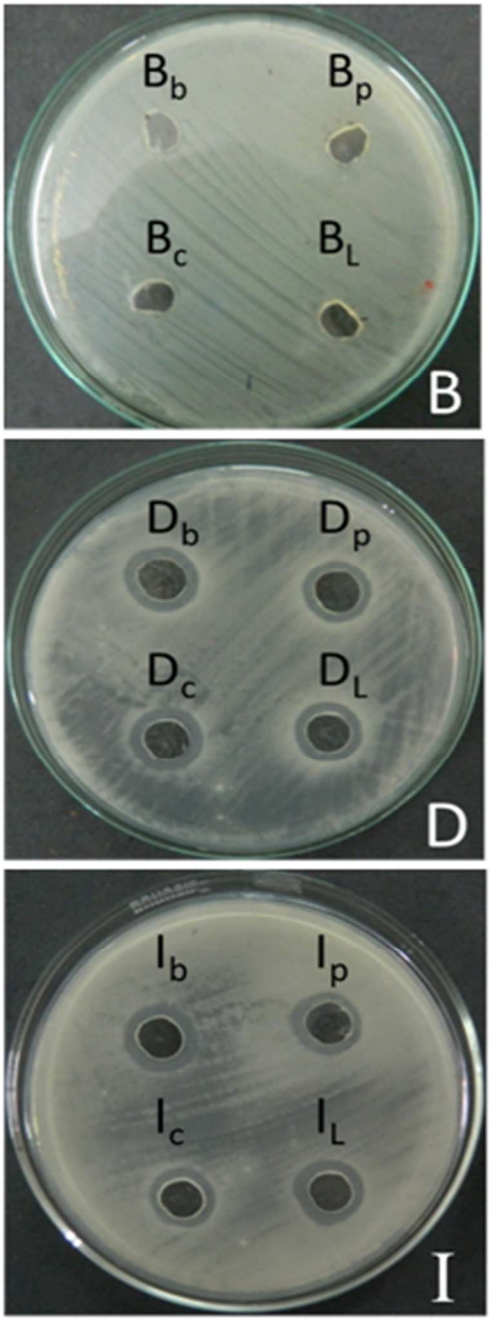

Fig. 10 Antibacterial effect of drug loaded NLC on the growth of *Bacillus amyloliquefaciens*. Systems: B, control; D, DNa and I, IMC. Subscripts: b, base-NLC; p, PEG coated; c, NaCMC coated and L, LM200 coated NLCs.

4. Conclusion

Effect of cationic (LM200), anionic (NaCMC) and nonionic (PEG) polymers as well as two drugs DNa and IMC were investigated on the physicochemical properties of NLCs. Concentration and charge of polymers as well as the drugs greatly controlled the NLC behavior. 0.01 wt% polymer in combination with 10 mM aqueous Tween 60 was the optimum condition in stabilizing the NLCs. Both the polymers and the drugs generated imperfection in the packing of the NLC components. NaCMC exhibited anomalous behaviour probably due to the similarity in the electrical charges with NLCs; the disorderdness was markedly reduced in case of LM200 stabilized systems. Higher entrapment efficiency was experienced by IMC due to its greater lipophilicity than DNa. Effect of polymer charge on IMC loading was insignificant unlike DNa. Drug release from the lipid matrix was dependent on the polymer; PEG and NaCMC enhanced the release whereas LM200 delayed the sutained release of both the drugs. While the release of IMC was diffusion controlled, a combined diffusion and dissolution controlled process was experienced by DNa. Systems were found to exhibit substantial antibacterial activies towards gram positive strains. Further characterizations using cryo-TEM, X-ray scattering and atomic force microscopic studies are warranted to finaly conclude about the systems. Besides, *in vivo* studies may be carried out which eventually would substantiate the potential of the systems as novel drug delivery agent with reduced toxicity for the conventional nonsteroidal anti-inflammetory drugs.

Acknowledgements

Financial assistance from the Department of Science and Technology, Govt. of India, in the form of a research grant (Ref No. SR/S1/PC/32/2011) is sincerely acknowledged. M.S. acknowledges the facilities from the University of North Bengal.

Author Information

[1]Department of Pharmaceutics, Himalayan Pharmacy Institute, Majhitar, Rangpo, East Sikkim – 737136, India
[2]Department of Chemistry, University of North Bengal, Darjeeling – 734013, West Bengal, India
[3]Department of Biotechnology, University of North Bengal, Darjeeling – 734013, West Bengal, India
[4]Department of Chemistry, Bose Institute, Kolkata 700009, West Bengal, India
[5]Department of Pure and Applied Chemistry, Tokyo University of Science, 2641 Yamazaki, Noda, Tokyo 278-8510, Japan

Notes and References

1 S. Das and A. Chaudhury, *AAPS Pharm. Sci. Tech.* 2011, **12**, 62-76.

2 B. J. Boyd, *Int. J. Pharm.* 2003, **260**, 239-247.

3 M. L. Lynch, A. Ofori-Boateng, A. Hippe, K. Kochvar and P. T. Spicer, *J. Colloid Interface Sci.* 2003, **260**, 404-413.

4 M. Nakano, A. Sugita, H. Matsuoka and T. Handa, *Langmuir* 2001, **17**, 3917-3922.

5 D. Prashar and D. Sharma, *Asian J. Res. Pharm. Sci.* **2**011, **1**, 59-62.

6 S. B. Rizwan, W. T. McBurney, K. Young, T. Hanley, B. J. Boyd, T. Rades and S. Hook, *J. Controlled Release* 2013, **165**, 16-21.

7 P. Spicer, *Chem. Eng. Res. Des.* 2005, **83**, 1283-1286.

8 P. T. Spicer, *ACS Symp. Ser.* 2003, **861**, 346-359.

9 P. T. Spicer, *Current Opin. Colloid Interface Sci.* 2005, **10**, 274–279.

10 P. T. Spicer, in *Book Cubosomes: Bicontinuous Liquid Crystalline Nanoparticles*, ed. by Editor, CRC Press, 2014, Vol. 2, pp. 1070-1080.

11 P. T. Spicer, K. L. Hayden, M. L. Lynch, A. Ofori-Boateng and J. L. Burns, *Langmuir* 2001, **17**, 5748-5756.

12 P. T. Spicer, W. B. Small, II, M. L. Lynch and J. L. Burns, *J. Nanopart. Res.* 2002, **4**, 297-311.

13 R. Hirlekar, S. Jain, M. Patel, H. Garse and V. Kadam, *Current Drug Deliv.* 2010, **7**, 28–35.

14 K. Larsson, *Proc. Int. Symp. Controlled Release Bioact. Mater.* 1997, **24**, 198-199.

15 D. Libster, A. Aserin, D. Yariv, G. Shoham and N. Garti, *Colloids Surf., B* 2009, **74**, 202-215.

16 W.-K. Fong, T. L. Hanley, B. Thierry, A. Tilley, N. Kirby, L. J. Waddington and B. J. Boyd, *Phys. Chem. Chem. Phys.* 2014, **16**, 24936-24953.

17 I. D. Mat Azmi, L. Wu, P. P. Wibroe, C. Nilsson, J. Oestergaard, S. Sturup, B. Gammelgaard, A. Urtti, S. M. Moghimi and A. Yaghmur, *Langmuir* 2015, **31**, 5042-5049.

18 J. Wang, F. Guo, M. Ma, M. Lei, F. Tan and N. Li, *RSC Adv.* 2014, *4*, 45458-45466.

19 F. Tamjidi, M. Shahedi, J. Varshosaz and A. Nasirpour, *Innov. Food Sci. Emerg. Technol.* 2013, **19**, 29-43.

20 G. Fricker, T. Kromp, A. Wendel, A. Blume, J. Zirkel, H. Rebmann, C. Setzer, R.-O. Quinkert, F. Martin and C. Müller-Goymann, *Pharm. Res.* 2010, **27**, 1469-1486.

21 S. Wissing, O. Kayser and R. Müller, *Adv. Drug Deliv. Rev.* 2004, **56**, 1257-1272.

22 J. Shan and H. Tenhu, *Chem. Commun.* 2007, 4580-4598.

23 T. Ramasamy, Z. S. Haidar, T. H. Tran, J. Y. Choi, J.-H. Jeong, B. S. Shin, H.-G. Choi, C. S. Yong and J. O. Kim, *Acta Biomater.* 2014, **10**, 5116-5127.

24 Y.-C. Kuo and J.-F. Chung, *Colloids Surf B:* 2011, **83**, 299-306.

25 K. Zheng, A. Zou, X. Yang, F. Liu, Q. Xia, R. Ye and B. Mu, *Food Hydrocolloids* 2013, **32**, 72-78.

26 K. Kawakami, Y. Nishihara and K. Hirano, *J. Phys. Chem. B* 2001, **105**, 2374-2385.

27 M. Garcıa-Fuentes, D. Torres and M. Alonso, *Colloids Surf. B:* 2003, **27**, 159-168.

28 T. Ramasamy, T. H. Tran, J. Y. Choi, H. J. Cho, J. H. Kim, C. S. Yong, H.-G. Choi and J. O. Kim, *Carbohydr. Polym.* 2014, **102**, 653-661.

29 V. K. Venishetty, R. Chede, R. Komuravelli, L. Adepu, R. Sistla and P. V. Diwan, *Colloids Surf. B:* 2012, **95**, 1-9.

30 M. J. Ernsting, W.-L. Tang, N. MacCallum and S.-D. Li, *Bioconjugate Chem.* 2011, **22**, 2474-2486.

31 E. Terada, Y. Samoshina, T. Nylander and B. Lindman, *Langmuir* 2004, **20**, 6692-6701.

32 C. Yiyun and X. Tongwen, *Eur. J. Med. Chem.* 2005, **40**, 1188-1192.

33 A. AL-Janabi, *Asian J. Pharm.* 2009, **3**, 148-152.

34 R. Polisson, *Am. J. Med.* 1996, **100**, 31S-36S.

35 T. Ramasamy, U. S. Khandasami, H. Ruttala and S. Shanmugam, *Macromol. Res.* 2012, **20**, 682-692.

36 R. Müller, M. Radtke and S. Wissing, *Adv. Drug Deliv. Rev.* 2002, **54,** S131-S155.

37 L. Zhao, J. Du, Y. Duan, Y. n. Zang, H. Zhang, C. Yang, F. Cao and G. Zhai, *Colloids Surf. B:* 2012, **97**, 101-108.

38 Y. Zhang, M. Huo, J. Zhou, A. Zou, W. Li, C. Yao and S. Xie, *AAPS J.* 2010, **12**, 263-271.

39 S. Majumder, B. Naskar, S. Ghosh, C.-H. Lee, C.-H. Chang, S. P. Moulik and A. K. Panda, *Colloids Surf. A:* 2014, **443**, 156-163.

40 W. Mehnert and K. Mäder, *Adv. Drug Deliv. Rev.* 2001, **47**, 165-196.

41 P. Guha, B. Roy, G. Karmakar, P. Nahak, S. Koirala, M. Sapkota, T. Misono, K. Torigoe and A. K. Panda, *J. Phys. Chem. B* 2015, **119**, 4251-4262.

42 P. Nahak, G. Karmakar, B. Roy, P. Guha, M. Sapkota, S. Koirala, C.-H. Chang and A. K. Panda, *RSC Adv.* 2015, **5**, 26061-26070.

43 R. I. El-Gogary, N. Rubio, J. T.-W. Wang, W. T. Al-Jamal, M. Bourgognon, H. Kafa, M. Naeem, R. Klippstein, V. Abbate and F. Leroux, *ACS nano* 2014, **8**, 1384-1401.

44 H. Yuan, L.-L. Wang, Y.-Z. Du, J. You, F.-Q. Hu and S. Zeng, *Colloids Surf. B:* 2007, **60**, 174-179.

45 A. Gole, S. Phadtare, M. Sastry and D. Langevin, *Langmuir* 2003, **19**, 9321-9327.

46 A. Panya, M. Laguerre, J. Lecomte, P. Villeneuve, J. Weiss, D. J. McClements and E. A. Decker, *J. Agric. Food Chem.* 2010, **58**, 5679-5684.

47 J. Luan, X. Yang, L. Chu, Y. Xi and G. Zhai, *J. Colloid Interface Sci.* 2014, **428**, 49-56.

48 M. Cohen-Avrahami, A. I. Shames, M. F. Ottaviani, A. Aserin and N. Garti, *Colloids Surf. B:* 2014, **122**, 231-240.

49 S. Souza, O. Oliveira Jr, M. Scarpa and A. Oliveira, *Colloids Surf. B:* 2004, **36**, 13-17.

50 P. Alexandridis and K. Andersson, *J. Colloid Interface Sci.* 1997, **194**, 166-173.

51 F. Guillemet and L. Piculell, *J. Phys. Chem.* 1995, **99**, 9201-9209.

52 Y. Chen, X. Yang, L. Zhao, L. Almásy, V. M. Garamus, R. Willumeit and A. Zou, *Colloids Surf. A:* 2014, **455**, 36-43.

53 A. B. Kovačević, R. H. Müller, S. D. Savić, G. M. Vuleta and C. M. Keck, *Colloids Surf. A:*2014, **444**, 15-25.

54 M. Garcia-Fuentes, D. Torres and M. J. Alonso, *Int. J. Pharm.* 2005, **296**, 122-132.

55 R. Duro, C. Alvarez, R. Martínez-Pacheco, J. L. Gómez-Amoza, A. Concheiro and C. Souto, *Eur. J. Pharm. Biopharm.* 1998, **45**, 181-188.

56 M. G. Carneiro-da-Cunha, M. A. Cerqueira, B. W. Souza, J. A. Teixeira and A. A. Vicente, *Carbohydr. Polym.* 2011, **85**, 522-528.

57 T. Waraho, V. Cardenia, Y. Nishino, K. N. Seneviratne, M. T. Rodriguez-Estrada, D. J. McClements and E. A. Decker, *Food Res. Intl.* 2012, **48**, 353-358.

58 J. Liu, T. Gong, C. Wang, Z. Zhong and Z. Zhang, *Int. J. Pharm.* 2007, **340**, 153-162.

59 D. Chapman, *J. Chem. Soc.* 1956, 2522-2528.

60 G. Cavallaro, G. La Manna, V. T. Liveri, F. Aliottav M. Fontanella, *J. Colloid Interface Sci.* 1995, **176**, 281-285.

61 A. Sar and A. Karaipekli, *Solar Energy Materials and Solar Cells* 2009, **93**, 571-576.

62 X. Shen, D. Yu, L. Zhu, C. Branford-White, K. White and N. P. Chatterton, *Int. J. Pharm.* 2011, **408**, 200-207.

63 C. Nunes, G. Brezesinski, C. Pereira-Leite, J. L. Lima, S. Reis and M. Lúcio, *Langmuir* 2011, **27**, 10847-10858.

64 S. H. Jin, S. H. Kim, H. N. Cho and S. K. Choi, *Macromolecules* 1991, **24**, 6050-6052.

65 K. J. Tangso, S. Lindberg, P. G. Hartley, R. Knott, P. Spicer and B. J. Boyd, *ACS Appl. Mater. Interfaces* 2014, **6**, 12363-.

66 S. Mehta, N. Bala and S. Sharma, *Colloids Surf. A:* 2005, **268**, 90-98.

67 M. Ricci, C. Puglia, F. Bonina, C. D. Giovanni, S. Giovagnoli and C. Rossi, *J. Pharm. Sci.* 2005, **94**, 1149-1159.

68 Y. Boonsongrit, A. Mitrevej and B. W. Mueller, *Eur. J. Pharm. Biopharm.* 2006, **62**, 267-274.

69 P. Piyakulawat, N. Praphairaksit, N. Chantarasiri and N. Muangsin, *AAPS PharmSciTech* 2007, **8**, 120-130.

70 E. R. Morris, A. Cutler, S. Ross-Murphy, D. Rees and J. Price, *Carbohydr. Polym.* 1981, **1**, 5-21.

71 A. Dan, S. Ghosh and S. P. Moulik, *Carbohydr. Polym.* 2010, **80**, 44-52.

72 J. E. Kristiansen, *APMIS. Supplementum* 1991, **30**, 7-14.